ELSEVIER

Journal of Wind Engineering
and Industrial Aerodynamics 96 (2008) 524–539

JOURNAL OF
wind engineering
AND
industrial
aerodynamics

www.elsevier.com/locate/jweia

Development of a shrouded wind turbine with a flanged diffuser

Yuji Ohya[a,*], Takashi Karasudani[a], Akira Sakurai[b], Ken-ichi Abe[b], Masahiro Inoue[c]

[a]*Research Institute for Applied Mechanics, Kyushu University, 6-1 Kasuga-koen, Kasuga 816-8580, Japan*
[b]*Department of Aeronautics and Astronautics, Kyushu University, Fukuoka 812-8581, Japan*
[c]*Sasebo National College of Technology, Sasebo 857-1193, Japan*

Received 28 August 2005; received in revised form 6 November 2006; accepted 11 January 2008
Available online 19 March 2008

Abstract

We have developed a wind turbine system that consists of a diffuser shroud with a broad-ring flange at the exit periphery and a wind turbine inside it. The flanged-diffuser shroud plays a role of a device for collecting and accelerating the approaching wind. Emphasis is placed on positioning the flange at the exit of a diffuser shroud. Namely, the flange generates a low-pressure region in the exit neighborhood of the diffuser by vortex formation and draws more mass flow to the wind turbine inside the diffuser shroud. To obtain a higher power output of the shrouded wind turbine, we have examined the optimal form of the flanged diffuser, such as the diffuser open angle, flange height, hub ratio, centerbody length, inlet shroud shape and so on. As a result, a shrouded wind turbine equipped with a flanged diffuser has been developed, and demonstrated power augmentation for a given turbine diameter and wind speed by a factor of about 4–5 compared to a standard (bare) wind turbine. In a field experiment using a prototype wind turbine with a flanged diffuser shroud, the output performance was as expected and equalled that of the wind tunnel experiment.

Keywords: Wind energy; Wind turbine; Flanged diffuser shroud; Wind tunnel experiment

*Corresponding author. Tel.: +81 92 583 7777; fax: +81 92 583 7779.
E-mail address: ohya@riam.kyushu-u.ac.jp (Y. Ohya).

0167-6105/$ - see front matter
doi:10.1016/j.jweia.2008.01.006

1. Introduction

For the application of an effective energy resource in the future, the limitation of fossil fuels is clear and the security of alternative energy sources is an important subject. Furthermore, as concerns for environmental issues, i.e., global warming, etc., the development and application of renewable and clean new energy are strongly expected. Among others, wind energy technologies have developed rapidly and are about to play a big role in a new energy field. However, in comparison with the overall demand for energy, the scale of wind power usage is still small; especially, the level of development in Japan is extremely small. As for the reasons, various causes are conceivable. For example, the limited local area suitable for wind power plants, the complex terrain compared to that in European or North American countries and the turbulent nature of the local wind are pointed out. Therefore, the introduction of a new wind power system that produces higher power output even in areas where lower wind speeds and complex wind patterns are expected is strongly desired.

Wind power generation is proportional to the wind speed cubed. Therefore, a large increase in output is brought about if it is possible to create even a slight increase in the velocity of the approaching wind to a wind turbine. If we can increase the wind speed by utilizing the fluid dynamic nature around a structure or topography, namely if we can concentrate the wind energy locally, the power output of a wind turbine can be increased substantially. Although there have been several studies of collecting wind energy for wind turbines reported so far (Lilley and Rainbird, 1956; Gilbert et al., 1978; Gilbert and Foreman, 1983; Igra, 1981; Phillips et al., 1999, 2000; Bet and Grassmann, 2003; Nagai and Irabu, 1987), it has not been an attractive research subject conventionally. Unique research that was carried out intensively in the past is the examination of a diffuser-augmented wind turbine (DAWT) by Gilbert et al. (1978), Gilbert and Foreman (1983), Igra (1981) and others around 1980. In their studies, there was a focus on concentrating wind energy in a diffuser with a large open angle; a boundary layer controlled with several flow slots was employed to realize a flow that goes along the inside surface of the diffuser. Thus, the method of boundary layer control prevents pressure loss by flow separation and increases the mass flow inside the diffuser. Based on this idea, a group in New Zealand (Phillips et al., 1999, 2000) developed the Vortec 7 DAWT. They used a multi-slotted diffuser to prevent separation within the diffuser. Bet and Grassmann (2003) developed a shrouded wind turbine with a wing-profiled ring structure. It was reported that their DAWT showed an increase in power output by the wing system by a factor of 2.0, compared to the bare wind turbine. Nagai and Irabu (1987) investigated a venturi-type structure, i.e., the front portion is a nozzle and the rear portion is a diffuser, as a structure concentrating the wind energy, especially paying attention to the effect of the diffuser part. He analyzed the flow inside the venturi-type structure using a momentum theory. Although several other ideas have been reported so far, most of them do not appear to be reaching commercialization.

The present study, regarding the development of a wind power system with high output, aims at determining how to collect the wind energy efficiently and what kind of wind turbine can generate energy effectively from the wind. For this purpose, we have developed a diffuser-type structure that is capable of collecting and accelerating the approaching wind. Namely, we have devised a diffuser shroud with a large flange that is able to increase the wind speed from approaching wind substantially by utilizing various flow characteristics, e.g., the generation of low-pressure region by vortex formation, flow entrainment by vortices and so on, of the inner or peripheral flows of a diffuser shroud equipped with a flange. Although it adopts a diffuser-shaped structure surrounding a wind turbine like the others (Lilley and Rainbird, 1956; Gilbert et al., 1978; Gilbert and Foreman, 1983; Igra, 1981; Phillips et al., 1999, 2000; ; Bet and Grassmann, 2003; Nagai and Irabu, 1987), the feature that distinguishes it from the others is a large flange attached at the exit of the diffuser shroud. Furthermore, we placed a wind turbine inside the diffuser shroud equipped with a flange and evaluated the power output generated. As a result, the shrouded wind turbine equipped with a flanged diffuser demonstrated power augmentation for a given turbine diameter and wind speed by a factor of about 4–5 compared to a standard micro wind turbine.

2. Wind tunnel experiment

The large boundary-layer wind tunnel of the Research Institute for Applied Mechanics, Kyushu University, was used. It had a 3.6 m wide $\times$ 2 m high $\times$ 15 m long measurement section and the maximum wind velocity was 30 m/s. Various hollow-structure models of the pyramid type or cone type were made of polystyrene, acrylic or aluminum plates. The models were hung and supported by strings in the center of the wind tunnel section. The distributions of wind velocity U and static pressure p along the central axis or periphery of the hollow-structure model were measured with an I-type hot-wire and a static-pressure tube using a traversing system. The static-pressure coefficient is defined as $C_p = (p - p_\infty)/(0.5\rho U_\infty^2)$, where U_∞ is the approaching wind speed, ρ is the air density, and p_∞ is the static pressure that corresponds to U_∞ in a far upstream position. The representative scale length of a model is the entrance width (or the entrance diameter) D of 12–60 cm, the wind velocity $U_\infty = 5$ m/s, and the Reynolds number $Re = 4 \times 10^4 - 1.3 \times 10^5$. In the case of using a big hollow-structure model, paying attention to the blockage effect in the wind tunnel, we removed the walls of the ceiling and both sides ranging 6 m in the center portion of the measurement section. Namely, we used our wind tunnel with an open-type test section to avoid the blockage effect. The smoke-wire technique was employed for the flow visualization experiment.

3. Development of a collection-acceleration device for wind (diffuser shroud equipped with a flange)

3.1. Selection of a diffuser-type structure as the basic form

We examined the inner flow of three typical hollow structures, as shown in Fig. 1; namely, a nozzle-type model that reduces the inside cross-section, a cylindrical-type model that has a constant inside cross-section and a diffuser-type model that expands the inside cross-section downstream. For both ends of the hollow-structure model, the narrow-end is a square cross-section of $D = 12$ cm and the wide end is $D = 24$ cm. The area ratios μ defined as the outlet area/inlet area of the three hollow-structure models are 1/4, 1 and 4 for the nozzle-, cylindrical- and diffuser-type models, respectively. For the nozzle and diffuser types, the angle of inclination φ is 3.7°. The length ratio $L/D = 7.7$, here, L is the model length.

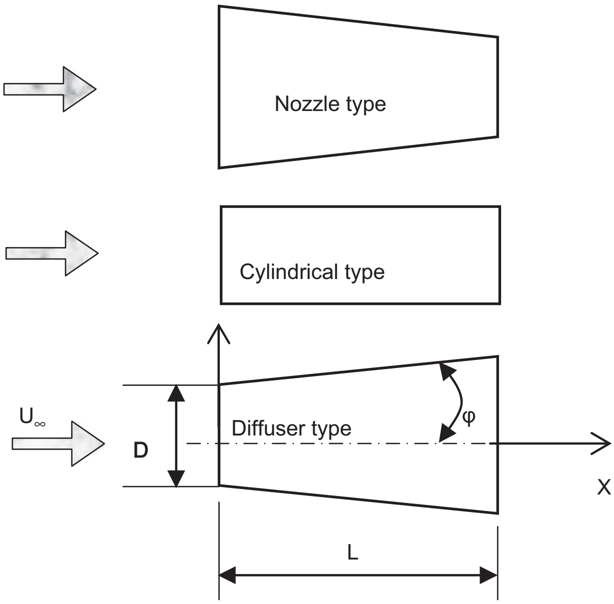

Fig. 1. Three types of hollow structures.

Figs. 2a and b show the wind velocity distribution U/U_∞ and static pressure distribution C_p on the central axis of a hollow-structure model. As seen in Fig. 2a, the diffuser model has a remarkable effect on the collection and acceleration of the approaching wind. A maximum of $U/U_\infty \sim 1.8$ is shown in the neighborhood immediately after the entrance. Here, $x/L = 0$ is the model entrance and $x/L = 1$ is the model exit. Figs. 3a and b show the flows inside and outside the nozzle- and diffuser-type models. The flow is from left to right. As seen in Fig. 3a, the wind tends to avoid the nozzle-type model, while the wind flows into the diffuser-type model as it is inhaled, as seen in Fig. 3b. Examining the optimal inclination angle φ (the half-open angle) of this diffuser, it is found that the angle φ of around 4° is most effective. Also, for the diffuser model, we examined the relationship between the maximum increase ratio (speed-up ratio) U_{max}/U (U_{max} is the maximum wind speed on the central axis) and the length ratio of L/D. Wind speed gradually increases with L/D, as shown in Fig. 4 (the case of diffuser only). Thus, it was confirmed that the diffuser structure is most effective for collecting and accelerating the wind.

3.2. Improvement of speed-up performance of the diffuser structure by the addition of periphery appendages

It was found that a remarkable increase in wind speed was obtained if a long diffuser body over $L/D = 3$ is used, as shown in Fig. 4 (the case of diffuser only). However, in the practical point of view, it is preferable to have a short diffuser body with a L/D of less than 2 that has similar performance to that of a long diffuser body. Therefore, we examined a short diffuser-type structure which is capable of providing more effective performance by applying various ideas to the short body (Ohya et al., 2002). A diffuser model with a

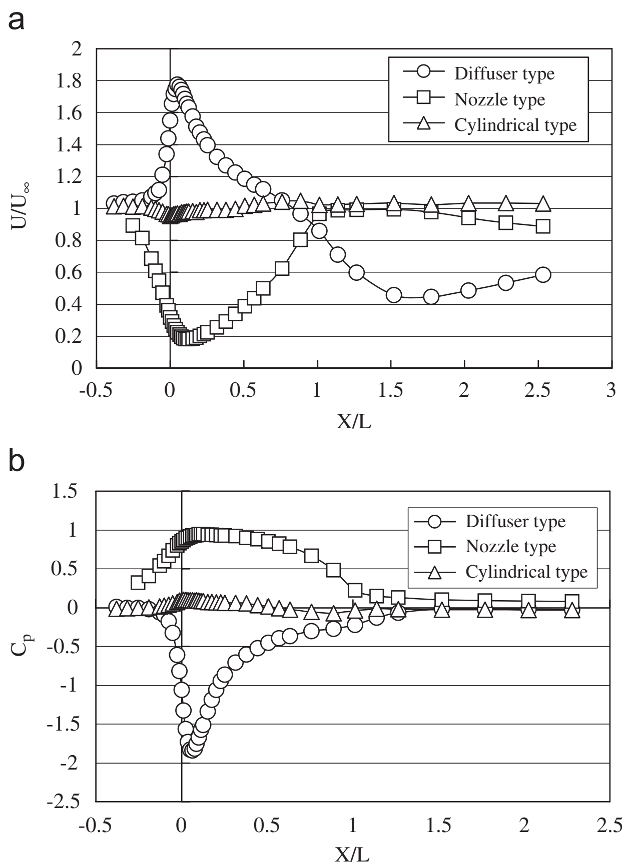

Fig. 2. Wind velocity and static pressure distributions on the central axis of a hollow structure, $L/D = 7.7$. The area ratios μ (outlet area/inlet area) of the three hollow-structure models are 1/4, 1 and 4 for the nozzle-, cylindrical- and diffuser-type models, respectively: (a) wind velocity and (b) static pressure.

square section of $D = 40\,\text{cm}$ and with a half-open angle $\varphi = 4^\circ$ was used in this experiment.

As a result of several attempts, it was found that wind speed is increased by adding an appropriate entrance (called an inlet shroud) and a ring-type flange at the exit periphery (see Figs. 5, 6, 8 and 9) to the diffuser body. The inlet shroud opening has a smooth curved surface surrounding the entrance of the diffuser model. The flange is a ring-type square plate with a height of $h = 10\,\text{cm}$ ($h/D = 0.25$), and is attached vertically to the outer periphery of the diffuser model at the exit. As shown in Fig. 4, when both the inlet shroud and the flange are employed, a remarkable increase in wind speed can be obtained, exceeding the case of a diffuser model only, and achieving a high velocity that is 1.6–2.4 times greater than that of the approaching wind velocity U_∞. For even a short diffuser ($L/D = 1.5$) with flange attached to the downstream edge, $U/U_\infty \sim 1.7$ was achieved.

The effect of the inlet shroud is found in the following point: It restrains flow separation at the entrance fairly well and the wind flows in more smoothly. Further examination of

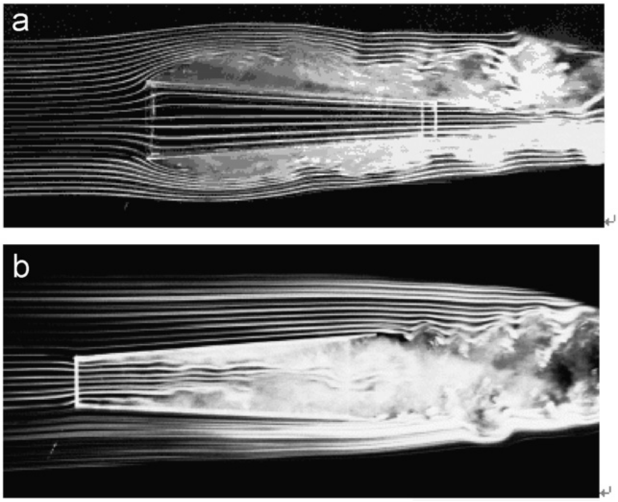

Fig. 3. Flows around a nozzle- and diffuser-type models. $L/D = 7.7$. The smoke flows from left to right: (a) nozzle-type model and (b) diffuser-type model.

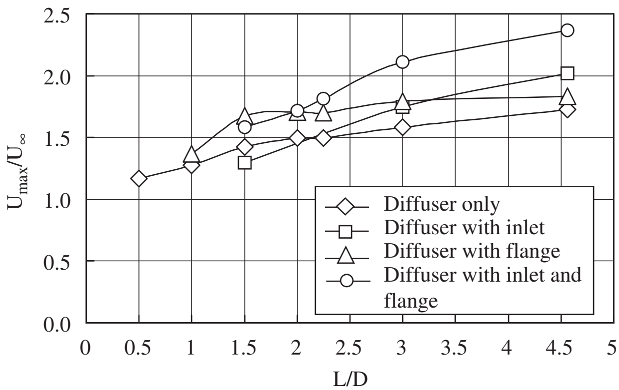

Fig. 4. Increase in the maximum wind velocity by the addition of an element to the diffuser-type model.

the inlet shroud was not conducted in the present experiment. In the next section, we discuss the mechanism that causes the wind to increase when using a flange.

Concerning the aforementioned experiments, although we mainly examined the acceleration performance using diffusers with square sections because of easier model production, we also examined diffusers with circular sections and found that they performed similar to that of the diffusers with square sections.

3.3. Mechanism of wind velocity acceleration

Here, we discuss the reason why the wind speed increases near the entrance when a large flange is attached to the outer periphery of a diffuser exit. Fig. 5 shows the visualization

Fig. 5. Flow around a circular-diffuser model with a flange. The smoke flows from left to right $L/D = 1.5$. The area ratio μ (outlet area/inlet area) of the circular-diffuser model is 1.44.

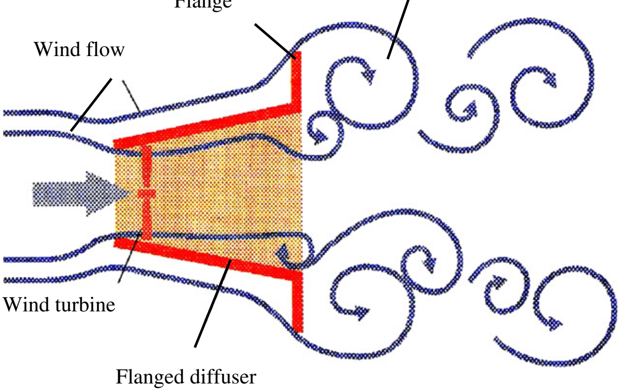

Fig. 6. Schematic view of flow mechanism around a flanged diffuser.

result of the flow around a circular diffuser ($D = 40$ cm) equipped with a flange using the smoke-wire technique. The flange used for the circular diffuser is a ring-type circular disk with a height of $h = 10$ cm ($h/D = 0.25$) and is attached to the outer periphery of the diffuser exit. The flow is from left to right. The vortex formation like the Karman vortex street is seen downstream of the flange. As shown in Fig. 7b (discussed later), owing to the vortex formation, the static base pressure p_b in the exit area at around $x/L = 1$ of the diffuser equipped with a flange falls to a fairly low pressure compared to that of the upstream flow p_∞, in comparison to the case of diffuser without a flange. The base-pressure coefficient at the exit of $x/L = 1$ is defined as $C_{pb} = (p_b - p_\infty)/(0.5\rho U_\infty^2)$. For the

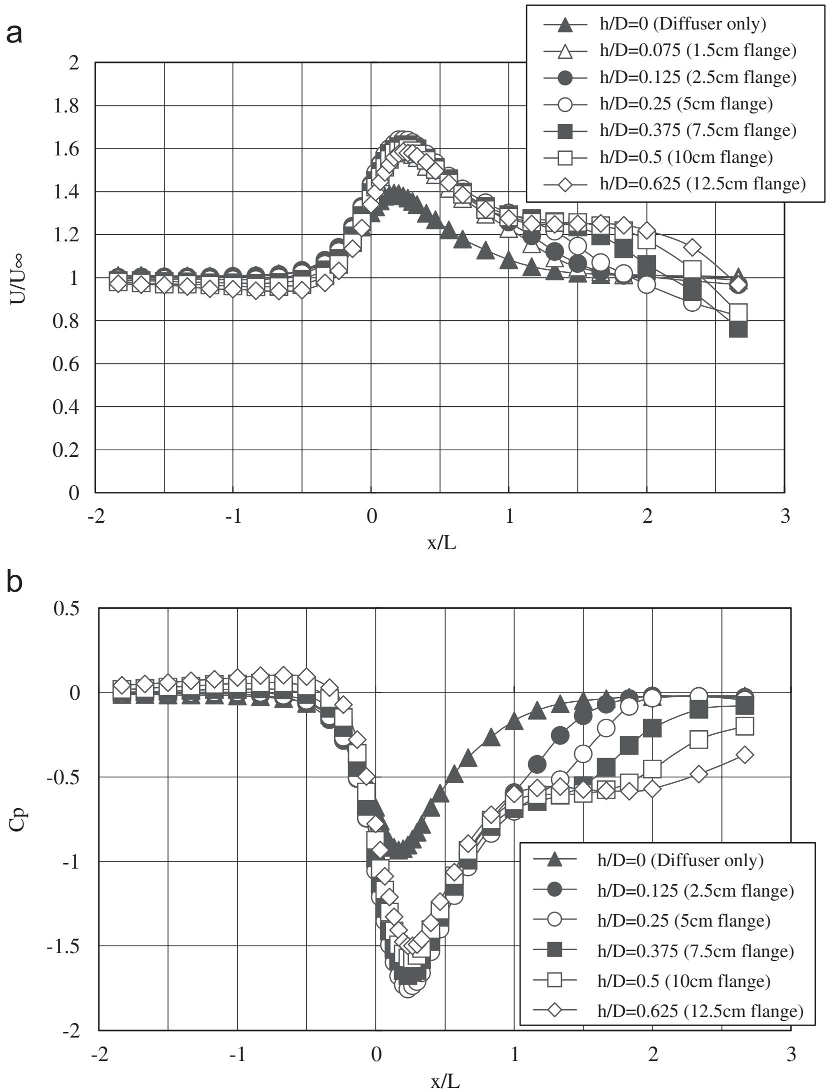

Fig. 7. Wind velocity and static pressure distributions on the central axis of a circular-diffuser model with and without a flange. $L/D = 1.5$. The area ratio μ of the circular-diffuser model is 1.44. (a) Wind velocity. (b) Static pressure.

diffuser without a flange, $C_{pb} = -0.2$. In contrast, for the diffuser equipped with a flange of $h/D = 0.25$, $C_{pb} = -0.75$.

From the smoke streaklines in Fig. 5, we can see that the approaching flow is inhaled into the diffuser near the entrance. Thus, the flange generates a low-pressure region in the near wake of the diffuser owing to the vortex formation and draws the flow into the diffuser. Fig. 6 illustrates an overview of the present wind-acceleration system. Generally, a flange may be thought to be an obstacle against the flow coming smoothly. However, this flange generates large size of separation behind it, where a low-pressure region appears to draw more wind compared to a diffuser with no flange. Owing to this effect, the flow coming into the diffuser can be effectively concentrated and accelerated.

3.4. Optimum size of the flange

We examined the optimum size of the flange to obtain the largest increase in wind speed near the diffuser entrance. The model used was a circular diffuser with $L/D = 1.5$ ($D = 20\,\text{cm}$). Circular flange of various heights of h were attached to the diffuser exit. Fig. 7 shows the wind velocity distribution U/U_∞ (Fig. 7a) and the static pressure distribution C_p (Fig. 7b) on the central axis. It was found that the flange of around $h/D = 0.25$ is most effective for the wind acceleration. From Fig. 7b, a flange larger than $h/D = 0.25$ causes a pressure increase in the upstream flow in front of the diffuser and prevents the approaching wind from smoothly flowing in. It should be noted that the most effective size of a flange is dependent on the diffuser length, L.

4. Demonstration experiment of wind power generation performance

4.1. Examination of the optimal flanged diffuser form with a wind turbine installed

Applying the flanged diffuser model to a small-size wind turbine, we examined the power output increase compared to a standard small wind turbine. Fig. 8 shows the experimental arrangement. It needs to be made into a compact structure to some degree if commercialization is to be realized. We used a short circular diffuser of $L/D = 1.25$ in this

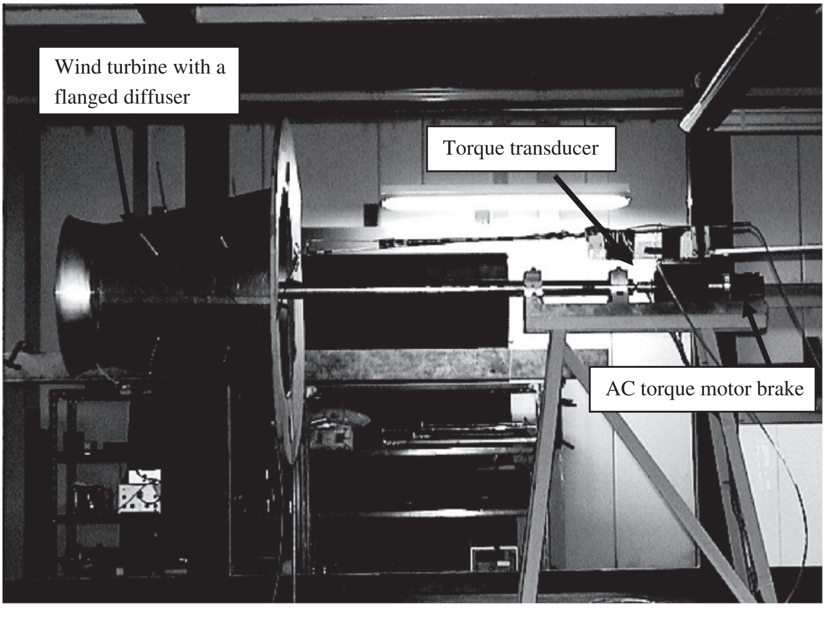

Fig. 8. Experiment on the power output generation of a wind turbine equipped with a flanged diffuser shroud.

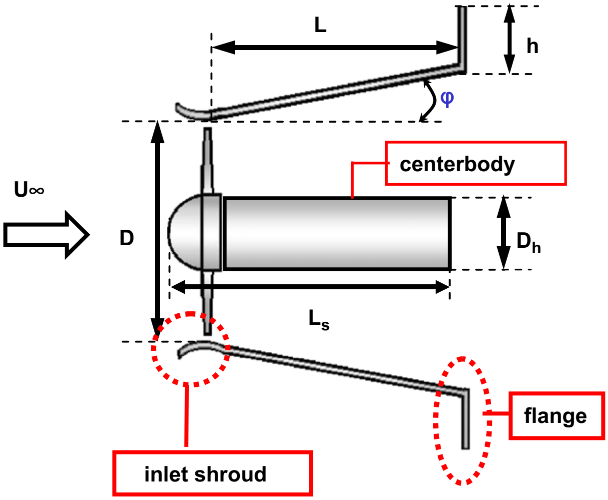

Fig. 9. Schematic of a wind turbine equipped with a flanged diffuser shroud.

demonstration experiment. The entrance diameter was $D = 60$ cm, and a flange height of $h/D = 0.5$ was adopted. As shown in Fig. 7, the optimal size of the flange is about $h/D = 0.25$ if a wind turbine is not installed inside the diffuser shroud. However, if a wind turbine is installed and works on the wind as a form of resistance, a larger flange of around $h/D = 0.5$ was effective for collecting and drawing the wind into the diffuser shroud.

Similarly, the diffuser opening angle φ (see Fig. 9) was changed from $\varphi = 4^\circ$ to 12°. It was found that when a wind turbine is installed in the diffuser entrance, it plays the role of a resistance body and controls separation of the flow inside the diffuser (Ohya et al., 2004). A numerical simulation also proved this. Abe and Ohya (2004) prepared a resistance screen model for their numerical model and examined how the flow inside the diffuser changes with the degree of the resistance screen. As a result, they showed that, in case of the resistance model, the flow separation near the diffuser entrance could be suppressed as the wind flows along the inner wall of the diffuser. Thus, the installation of a wind turbine reduces wind energy and works as a resistance body to the wind. For another reason, it seems that the diffuser becomes more efficient due to the additional swirl mixing mechanism, which increases boundary-layer momentum exchange. Therefore, this makes the adoption of a wider diffuser opening angle possible and leads to an improvement in the pressure recovery coefficient of the diffuser. This is an important parameter for shrouded wind turbine with flanged diffusers (Inoue et al., 2002).

Furthermore, we examined other shape parameters of the flanged diffuser such as the inlet shroud, hub ratio, centerbody length and so on, as illustrated in Fig. 9. Finally, we adopted a hub ratio $D_h/D = 22\%$ and the centerbody length $L_s = 0.75L$ (Ohya et al., 2004). Thus, the optimal shape for the flanged diffuser shroud used with a wind turbine has been found.

4.2. Output performance test of a wind turbine with a flanged diffuser shroud

As for the experimental method, a torque transducer (the rating 5 N m) was connected to the wind turbine and an AC torque motor brake was set behind it for the loading.

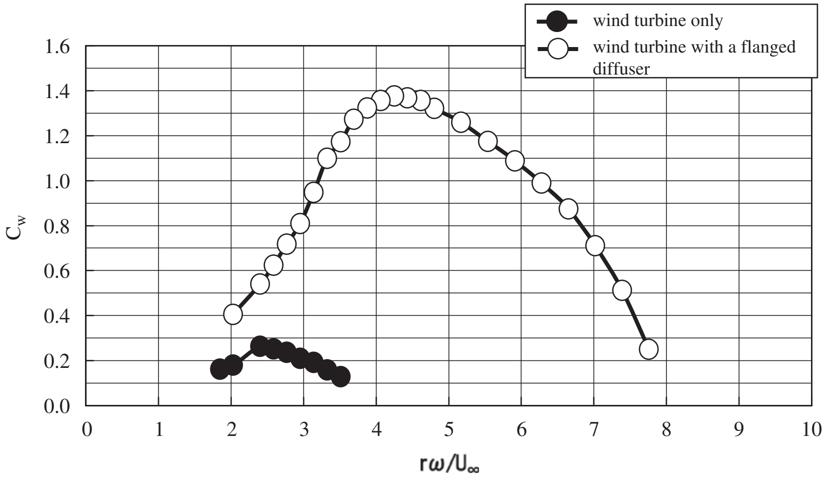

Fig. 10. Comparison of power coefficients between the wind turbine equipped with a flanged diffuser and the standard (bare) wind turbine. The area ratio μ (outlet area/inlet area) of the diffuser model is 2.35.

We measured the torque Q (N m) and the rotational speed n (Hz) of the wind turbine under the condition of gradually increasing the turbine load from zero. The calculated power output P (W) $= Q \times 2\pi n$ is shown as a performance curve. A wind turbine with a flanged diffuser shroud was supported by a long straight bar from the measurement bed, which was placed downstream and consisted of a torque transducer, a revolution sensor and an AC torque motor brake, as shown in Fig. 8. The approaching wind speed U_∞ was 6 m/s and the representative scale length equalled the diffuser entrance diameter D (= 60 cm) giving a Reynolds number $Re = 2.4 \times 10^5$.

Fig. 10 shows the experimental results. The horizontal axis shows the blade-tip-speed ratio $\lambda = \omega r/U_\infty$. Here, ω is the angular frequency, $2\pi n$, and r is the radius of a wind turbine rotor ($r = 0.294$ m). The vertical axis shows the power coefficient C_w ($= P/(0.5\rho U_\infty^3 A)$; where, A is the rotational area of the wind turbine rotor, πr^2). A wind turbine blade with NACA63-2 wing section contour was designed using a three-bladed wind turbine, resulting in an optimum tip-speed ratio of 5.0. As shown in Fig. 10, when a flanged diffuser is applied, a remarkable increase in the output power coefficient of approximately 5 times that of a conventional (bare) wind turbine is achieved. Namely, the C_w is 0.26 for a bare wind turbine, on the other hand, the C_w is 1.38 for a wind turbine with a flanged diffuser. The experimental results shown in Fig. 10 were obtained under the same wind speed and swept area of a wind turbine. It should be noted that, in the present experiment, the wind turbine rotor used is very small (the rotor diameter is 0.59 m), therefore the local chord of a blade leads to a low Reynolds number. The poor performance of the rotor ($C_w = 0.26$) seems to be related to Reynolds number effects.

To investigate the increase in wind velocity when the flanged diffuser is applied or not, the mean wind velocity U distributions in the radial direction in front of the rotating plane of blades were measured at each optimal tip-speed ratio ($\lambda = 4.2$ for the wind turbine equipped with a flanged diffuser and $\lambda = 2.5$ for the wind turbine only) using an I-type hot-wire with an anemometry. Fig. 11 shows the comparison of wind velocity distributions in the blade (radial) direction between the wind turbine equipped with a flanged diffuser

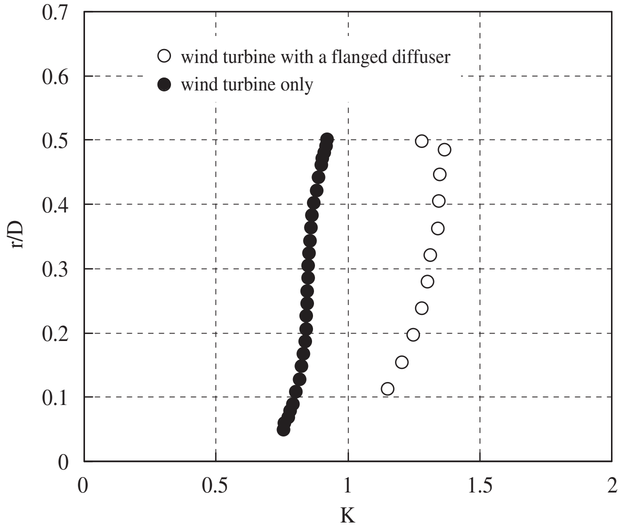

Fig. 11. Comparison of wind velocity distributions in the blade (radial) direction between the wind turbine equipped with a flanged diffuser and the wind turbine only. The mean velocity U was measured in front of the rotating plane of blades at each optimal tip-speed ratio ($\lambda = 4.2$ for the wind turbine equipped with a flanged diffuser and $\lambda = 2.5$ for the wind turbine only). K is the velocity ratio (wind speed-up ratio) of U/U_{∞}. r is the distance from the central axis of the wind turbine. D is the throat diameter of the diffuser as shown in Fig. 9.

and the wind turbine only. In the horizontal axis, K is the local velocity ratio (local wind speed-up ratio) of U/U_{∞}. In the vertical axis, r is the distance from the central axis of the wind turbine. D is the throat diameter of the diffuser as shown in Fig. 9. For the wind turbine with a flanged diffuser, K is around 1.3 as a spatial average in front of the blade-rotating plane. On the other hand, for the wind turbine only (without a flanged diffuser), K is around 0.8. The cubic value of $(1.3/0.8)^3$ almost reaches 4.3. This is consistent with the 4–5 times increase in the output power as shown in Fig. 10.

5. Field experiment on a prototype wind turbine with a flanged diffuser shroud

Fig. 12 shows the first prototype of a shrouded wind turbine equipped with a flanged diffuser (500 W class). The diffuser length of this prototype is 1.25 times as long as the diameter of the diffuser entrance D ($L = 1.25D$, $D = 0.72$ m). The height of the flange h is $0.5D$. The rotor diameter is 0.7 m.

To demonstrate the performance of a new wind turbine, we conducted a field experiment on a prototype shrouded wind turbine with a flanged diffuser. A shrouded wind turbine was placed on the top of a tower with a height of 8 m, as shown in Fig. 13. The wind speed was monitored with a three-cup anemometer, which was placed 1 m below the wind turbine. Fig. 14 shows the field experimental result measured on a windy day. The output power P (W) evaluated as 10 min averaged values are shown with the averaged wind speed U (m/s). As shown in Fig. 14, the averaged output data are plotted almost along the power curve of $C_w = 1.4$ obtained from the wind tunnel experiment. Thus, in a field experiment using the prototype wind turbine with a flanged diffuser, the performance was as expected

Fig. 12. Prototype wind turbine with a flanged diffuser shroud (500 W class). The rotor diameter is 0.7 m. $D = 0.72$ m. The area ratio μ (outlet area/inlet area) of the diffuser is 2.35.

and equalled that of the wind tunnel experiment. This supports that the present wind tunnel experiment is free from blockage effect.

Through the field experiment, it was found that the important features of this wind turbine equipped with a flanged diffuser are as follows:

(1) Four to five times increase in output power as compared with conventional wind turbines due to concentration of the wind energy.
(2) *Flange-based yaw control*: The flange at the exit of the diffuser makes wind turbines equipped with a flanged diffuser rotate following the change in the wind direction, like a weathercock. As a result, the shrouded wind turbine automatically turns to faces the wind.
(3) *Significant reduction in wind turbine noise*: Since the vortices generated from the blade tips are considerably suppressed through the interference with the boundary layer within the diffuser shroud, the aerodynamic noise is reduced substantially (Abe et al., 2005, 2006).
(4) *Improved safety*: The wind turbine, rotating at a high speed, is shrouded by a structure and is also safe against damage from broken blades.

6. Conclusions

We have developed a DAWT that can obtain a remarkably higher power output compared to conventional wind turbines.

Fig. 13. Prototype wind turbine with a flanged diffuser shroud in the field experiment (500 W class). The wind speed meter and wind direction meter were set 1 m below the wind turbine.

First, we examined a wind collection-acceleration device that makes it possible to concentrate the wind energy (i.e., increase the wind velocity locally and draw the wind to a wind turbine). It was confirmed that a hollow-structure diffuser is as effective as the shroud form for collecting and accelerating the wind.

To obtain a further increase in wind speed inside the diffuser shroud, a flange of proper height is attached to the outer periphery of the diffuser exit, successfully realizing a remarkable increase in wind speed of 1.6–2.4 times that of the approaching wind speed. This is because the flange generates a low-pressure region in the exit area of the diffuser by vortex formation and draws the wind into the diffuser.

Based on this idea of a flanged diffuser, we conducted a demonstration experiment of power generation of a shrouded wind turbine with a flanged diffuser both in the wind tunnel and field experiments. To obtain a higher power output of the shrouded wind turbine, we investigated the optimal form of the flanged diffuser with a wind turbine installed. Namely, we examined various shape parameters of the flanged diffuser such as the diffuser opening angle, flange height, hub ratio, centerbody length, inlet shroud and so on. As a result, the wind turbine equipped with a flanged diffuser shroud demonstrated

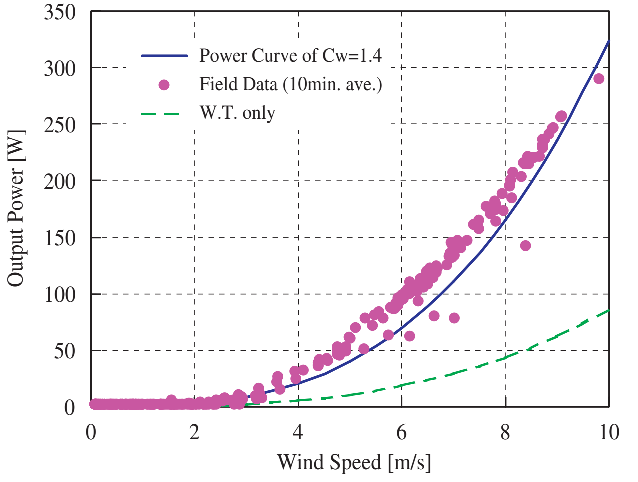

Fig. 14. Power output P vs. wind speed U in the field experiment for 500 W class. The solid line indicates the output power curve of $C_w = 1.4$ for the wind turbine equipped with a flanged diffuser as expected from the wind tunnel experiment. The broken line indicates the output power curve of $C_w = 0.35$ for the wind turbine only (without a flanged diffuser) as expected from the wind tunnel experiment. The dotted symbols indicate the measured data evaluated as 10 min average values on a windy day.

power augmentation for a given turbine diameter and wind speed by a factor of about 4–5 compared to a standard (bare) wind turbine.

Incidentally, owing to the existence of the flange, the shrouded wind turbine rotates in the horizontal plane and always faces in the direction of the approaching wind. Thus, the yawing motion is automatically controlled by the flange. Furthermore, application of the diffuser shroud results in a significant reduction of the wind turbine noise (blade-tip noise) and improves safety against broken blades.

Acknowledgments

This work was supported by four organizations including a Grant-in-Aids for Scientific Research, no. 14205139, sponsored by the Ministry of Education, Culture, Sports, Science and Technology, Japan, Environment Protection Research sponsored by the Sumitomo Fund, Fluid Machinery Research sponsored by the Harada Memorial Fund, and the Program and Project for Education and Research of Kyushu University. It was also supported by a matching fund from the Ministry of Economy, Trade and Industry. We gratefully acknowledge our laboratory staff, Messrs. N. Fukamachi and K. Watanabe, Research Institute for Applied Mechanics, Kyushu University, for their great cooperation in the experiments and data analysis.

References

Abe, K., Ohya, Y., 2004. An investigation of flow fields around flanged diffusers using CFD. J. Wind Eng. Ind. Aerodyn. 92, 315–330.

Abe, K., Nishida, M., Sakurai, M.A., Ohya, Y., Kihara, H., Wada, E., Sato, K., 2005. Experimental and numerical investigations of flow fields behind a small-type wind turbine with flanged diffuser. J. Wind Eng. Ind. Aerodyn. 93, 951–970.

Abe, K., Kihara, H., Sakurai, A., Nishida, M., Ohya, Y., Wada, E., Sato, K., 2006. An experimental study of tip-vortex structures behind a small wind turbine with a flanged diffuser. Wind Struct., 413–417.

Bet, F., Grassmann, H., 2003. Upgrading conventional wind turbines. Renew. Energy 28, 71–78.

Gilbert, B.L., Foreman, K.M., 1983. Experiments with a diffuser-augmented model wind turbine. Trans. ASME, J. Energy Resour. Technol. 105, 46–53.

Gilbert, B.L., Oman, R.A., Foreman, K.M., 1978. Fluid dynamics of diffuser-augmented wind turbines. J. Energy 2 (6), 368–374.

Igra, O., 1981. Research and development for shrouded wind turbines. Energy Convers. Manage. 21, 13–48.

Inoue, M., Sakurai, A., Ohya, Y., 2002. A simple theory of wind turbine with a flanged diffuser. Turbomachinery 30 (8), 497–502 (in Japanese).

Lilley, G.M., Rainbird, W.J., 1956. A preliminary report on the design and performance of ducted windmills. Report No. 102, College of Aeronautics, Cranfield, England.

Nagai, M., Irabu, K., 1987. Momentum theory for diffuser augmented wind turbine. Trans. JSME 53 (489), 1543–1547 (in Japanese).

Ohya, Y., Karasudani, T., Sakurai, A., 2002. Development of high-performance wind turbine with a brimmed diffuser. J. Japan Soc. Aeronaut. Space Sci. 50 (587), 477–482 (in Japanese).

Ohya, Y., Karasudani, T., Sakurai, A., 2004. Development of high-performance wind turbine with a brimmed diffuser—Part 2. J. Japan Soc. Aeronaut. Space Sci. 52 (604), 210–213 (in Japanese).

Phillips, D.G., Flay, R.G.J., Nash, T.A., 1999. Aerodynamic analysis and monitoring of the Vortec 7 diffuser augmented wind turbine. In: IPENZ Transactions, vol. 26(1), Auckland, New Zealand, pp. 13–19.

Phillips, D.G., Richards, P.J., Flay, R.G.J., 2000. CFD Modelling and the development of the diffuser augmented wind turbine. In: Proceedings of the Computational Wind Engineering 2000, 2000, Birmingham, pp. 189–192.